BIODIVERSITAS
Volume 23, Number 8, August 2022
Pages: 4223-4233

ISSN: 1412-033X
E-ISSN: 2085-4722
DOI: 10.13057/biodiv/d230846

Isolation and characterization of *IbAE7-like 1* gene encoding the cytosolic iron-sulfur cluster assembly pathway in response to skinning injury in sweetpotato

JOLLANDA EFFENDY♥
Department of Plant Breeding, Faculty of Agriculture, Universitas Pattimura. Jl. Ir. M. Putuhena, Poka Campus, Ambon 97233, Maluku, Indonesia.
Tel.: +62-911-322499, ♥email: jeffendy@alumni.sfu.ca

Manuscript received: 10 April 2022. Revision accepted: 1 August 2022.

Abstract. *Effendy J. 2022. Isolation and characterization of* IbAE7-like 1 *gene encoding the cytosolic iron-sulfur cluster assembly pathway in response to skinning injury in sweetpotato. Biodiversitas 23: 4223-4233.* Skinning injury is a major constrain in postharvest loss in sweetpotato due to the loss of skin from the surface of the roots. *ASYMMETRIC LEAVES1/2 ENHANCER7* (*AE7*) is an important cytosolic iron-sulfur (Fe-S) protein assembly (CIA) pathway. A partial cDNA *IbI51* encoding *AE7-like 1* was isolated from a skinning injury cDNA library to evaluate its potential role in response to skinning injury. The open reading frame of *IbAE7-like 1* consisted of 324 nucleotides and the deduced polypeptide sequences consisted of 108 amino acids with missing 46 amino acid residues at 5′ end. The amino acid sequence of IbAE7-like 1 shared 100% identity to AE7-like 1 previously identified in *Ipomoea triloba* and *Ipomoea nil* and 89.91-100% identity from other plants species. The findings indicated that AE7-like 1 was highly conserved in *Ipomoea* sp. In addition to similarity to AE7-like 1, IbAE7-like 1 also showed similarities to MIP18 (89.91-93.52%); DUF59 (91.67%); FAM96B (90.74%); and proteins with unknown function (90.74-91.67%). *IbAE7-like 1* mRNA transcripts showed transient expression in response to skinning injury. The phylogenetic analysis classified IbAE7-like 1 into three main classes. This study revealed *IbAE7-like 1* may play a key role in plant defense and wound repair to prevent DNA damage due to skinning injury in storage roots of sweetpotato.

Keywords: Cysteine residues, *Ipomoea batatas*, iron-sulfur, storage root, wounding

INTRODUCTION

Exogenous and endogenous genotoxic stressors are continually present in eukaryotic genomes, and these pressures commonly cause DNA damage. The *Arabidopsis thaliana* gene *ASYMMETRIC LEAVES1/2 ENHANCER7* (*AE7*) encodes a protein that is found in a wide range of eukaryotic species, from unicellular yeasts to humans. Although protein AE7 is assumed to be a key component of the cytosolic iron-sulfur (Fe-S) protein assembly (CIA) pathway, protein AE7-like 1 and 2 (both of which possess this domain) are unlikely to be involved (Luo et al. 2012).

Iron-sulfur (Fe-S) clusters have been identified as cofactors in several proteins essential for DNA repair and/or replication (Fuss et al. 2015). Small inorganic protein cofactors, Fe–S clusters serve as electron carriers in redox processes, catalysts in chemical reactions, regulatory sensors of environmental variables, sulfur donors for other cofactors, and devices for protein domain and genome stability (Lanz and Booker 2012; Paul and Lill 2015). Fe-S proteins are present in the mitochondria, cytosol, and nucleus of eukaryotic cells (Andreini et al. 2017; Lill 2020). Fe-S proteins have a role in a variety of activities, including mitochondrial energy generation, amino acid biosynthesis, cofactor biosynthesis, tRNA modification, and many aspects of protein translation as well as DNA creation and maintenance (Lill et al. 2015a; Lill et al. 2015b; Piccioli 2018; Lill and Freibert 2020; Shi et al. 2021). Recent research has made significant progress in our knowledge of how Fe-S clusters are assembled and inserted into cytosolic and nuclear target proteins. Furthermore, the synthesis of Fe–S clusters is connected to the stability of the nuclear genome (Paul and Lill 2015).

Several RNA-imaging methods, including differential-display reverse transcription polymerase chain reaction (DDRT-PCR) techniques, have previously been utilized as a first step in identifying differentially expressed genes (DEGs) under salt stress treatments in tomato roots (Wei et al. 2000; Babajani et al. 2009); ripening related pectin methylesterase inhibitor in banana fruit (Srivastava et al. 2012); MYB gene associated with calyx persistence in Korla fragrant pear (Wang et al. 2014); and seed development in *Carya cathayensis* Sarg. (Huang et al. 2015). To isolate DEGs, however, it is usually preferable to use a simple PCR-based sensitive yet reproducible technique that requires highly specific and short arbitrary primers. A recently designed technique used to identify differences in gene expression based on PCR is established by Hwang et al. (2003) and is known as GeneFishing™. GeneFishing™ is an innovative primer design known as the annealing control primer (ACP) method, which offers an effective primer with annealing specificity that selectively targets sequence hybridization to the template via a polydeoxyinosine poly(dI) linker (Hwang et al. 2003; Lee et al. 2012). The ACP technology approach is based on a unique tripartite structure of a particular oligo-nucleotide primer with its 30 and 50 ends divided by a regulator, and the interaction of each end of this primer during a two-

stage PCR. The use of the ACP to DEG identification yields reproducible, accurate, and lengthy (100 bp to 2 kb) PCR products visible on agarose gels due to the high annealing specificity during PCR. This technique has been used to identify abundant, transient, and rarely expressed candidate genes induced in response to skinning injury in sweetpotato (Effendy et al. 2013; Effendy et al. 2019); *Blumeria graminis* f. sp. *tritici* (*Bgt*) in wheat (Song et al. 2014); *Ralstonia solanacearum* phylotype I strain in *Solanum* lines (Baichoo et al. 2016); hypoxia in mouse embryonic stem cell (Hwang and Lee 2021). In this study, the ACP technology was used to isolate and characterize a sweetpotato partial cDNA clone encoding *IbAE7-like 1*. This novel *IbAE7-like 1* may play key roles in plant defense and wound repair to prevent DNA damage in response to skinning injury in storage roots of sweetpotato. The cDNA sequences, similarity, and phylogenetic analysis among related genes are also discussed in this paper.

MATERIALS AND METHODS

Plant materials

As described in Effendy et al. (2013; 2019), sweetpotato storage roots cultivar LA 07-146 that were freshly reaped, were cleansed, blotted, and scraped with a razor scraper (Titan 11030; Star Asia-USA, Renton, WA) to exfoliate the thin exterior pigmented skin. The roots were skinned and peeled to the same thickness (1.2 mm) at 0, 2, 4, 8, and 12 hours after skinning, with the peels subsequently frozen in liquid nitrogen and preserved at -80^{o}C for RNA extraction. As replicates, three individual roots were selected for each time point.

RNA isolation, cDNA preparation and ACP-based gene-fishing PCR

Total RNA was isolated using the RNeasy Mini Kit (Qiagen, Valencia, CA) according to the manufacturer guidelines (Effendy et al. 2013; Effendy et al. 2019). A spectrophotometer (ND-1000; Nanodrop Technologies, Wilmington, DE) was used to measure the quantity and quality of total RNA. To identify unique transcripts that may have escaped in one of the replicates due to technical faults during the GeneFishing^{TM} research, an aliquot of 2 µg RNA from three biological replicates isolated from storage root tissues for each time point was pooled. In addition, 3 µg RNA isolated from storage roots at 8 and 12 h was pooled to form a four-sample size for efficiency of PCR handling during gene fishing.

As reported previously by Effendy et al. (2013; 2019), a GeneFishing^{TM} DEG premix kit (Seegene, Rockville, MD) was used to synthesize first-strand cDNA synthesis. At each time course experiment, an aliquot of 3 µg RNA isolated from storage roots from independent replicates was pooled, with the exception of 8 h and 12 h, which were pooled together. The GeneFishing^{TM} DEG premix kit instructions from Seegene, Rockville, MD, were used to complete second strand cDNA synthesis and following PCR amplification in a single tube (Lee et al. 2012; Effendy et al. 2013; Effendy et al. 2019). During the second-stage PCR, twenty ACP primers were utilized, and further PCR amplification was undertaken in a single tube utilizing the GeneFishing^{TM} technique. DEG premix kit manual (Seegene, Rockville, MD) was used to capture DEGs in this study.

Cloning of Differentially Expressed Genes (DEGs)

The fragments belonging to DEGs were excised and extracted according to the manufacturer guidelines (QIAquick® Gel Extraction Kit Qiagen, Valencia, CA) depending on the presence/absence or relative intensity of ACP-PCR products between control and skinning samples. The DEGs were then cloned into the pGEM®-T Easy vector (Promega, Madison, WI) after being sliced from the gel. Colony PCR was utilized to confirm the nucleotide sequence of positive colonies from DEGs using the M13 reverse (5′-CAGGAAACAGCTATGACC-3′) and M13 forward (5′-GTAAAACGACGGCCAGT-3′) universal primers. In an ABI 3730xI DNA Analyzer, plasmids extracted from these clones were single-pass sequenced with T7 primer as per the manufacturer's guidelines.

Nucleotide and deduced amino acid sequencing analyses of DEGs

The vector backbone and poly (A) tail were manually removed from DNA sequences before being searched against NCBI's nonredundant nucleotide and protein database using the BLASTN and BLASTX interface (Altschul et al. 1997). The positive cDNA clone that was found to be similar to *AE7-like 1* was given the name *IbAE7-like 1* and was used for further studies. A total of 100 BLASTX matches that were similar to IbAE7-like 1 were grouped based on the type of genes and the number of occurrences of each gene, as well as similarity to AE7-like 1 for *Ipomoea* sp. The ClustalW program (Larkin et al. 2007) was used to align and compare sequences in order to spot homologs and estimate the functions of differentially expressed gene products in order to construct multiple sequence alignment in which three samples were chosen to represent each gene. The NCBI ORF Finder (http://www.ncbi.nlm.nih.gov/gorf/gorf.html) was used to predict the open reading frame and protein. BioEdit Sequence Alignment Editor was used to identified conserved amino acid sequences (Hall 1999). Using the bootstrap method with 1,000 bootstrap iterations, the unrooted phylogenetic tree was constructed from the deduced amino acid sequences for IbAE7-like 1 and other AE7-like 1 homologs from other *Ipomoea* species and other genes from other plants that exhibited similarities. The branching sequence is displayed in this tree, but the root or location of the last common ancestor is not specified. The phylogenetic tree was built using FigTree v1.4.3.x (Rambaut 2017) and the.dnd file generated in ClustalX2 (Larkin et al. 2007).

RESULTS AND DISCUSSION

Isolation and analysis of a candidate partial cDNA using ACP GeneFishing

The GeneFishing technology was used to identify genes that are differentially expressed during skinning injury by using total RNA isolated from freshly harvest storage roots exposed to skinning injury at 0, 2, 4, and combined (8 + 12) h. The impact of skinning injury on storage root RNA population was analyzed, and the speed with which changes in mRNA population occurred after skinning injury was quantified and used for ACP-PCR. An ACP18 primer was used in the experiments resulted in amplification of DEGs in storage roots in response to skinning injury. Based on the differential expression level of mRNA fragments observed on agarose gel, a DEG of interest was isolated and namely *IbI51*. *IbI51* showed higher expression at 0 + 4 h, and decreased at 2 and (8 + 12) h (Figure 1). This result showed that upon the onset of skinning injury, *IbI51* mRNA transcripts were transiently regulated. Rapid induction of *IbI51* mRNA at 4 h might indicate its involvement in DNA replication and/or repair (Luo et al. 2012).

Identification of a cDNA encoding *AE7-like 1* from storage roots of sweetpotato

An ACP18 primer used in the experiment showed changes in the amplification of DEG in storage roots after skinning injury at 0, 2, 4, (8 + 12) h. A cDNA clone was isolated and its sequence was determined. The cDNA product of interest was excised, re-amplified and then cloned. The insert of cDNA clone was sequenced and submitted to the NCBI server for comparison. Based on BLASTN search, *IbI51* showed similarity to *AE7-like 1* and namely *IbAE7-like 1*.

Without and with the exception of the deletions and substitutions of few nucleotides, analysis of the 3′ untranslated region (UTR) of the *IbAE7-like 1* cDNA clone with *InAE7-like 1* and *ItAE7-like 1* revealed a very high identity (98.7% and 98.2% identity) among these clones (Figure 2). The 3′ UTR of *IbAE7-like 1*, *InAE7-like 1* and *ItAE7-like 1* are almost identical except *InAE7-like 1* has additional one nucleotide T at position of 768 (Figure 2).

3' UTRs have been classed as new posttranscriptional regulatory elements since they have been found to regulate gene expression in bacteria by affecting mRNA stability and translation in both trans and cis (Ruiz de los Mozos et al. 2013; Laalami et al. 2014; Zhao et al. 2018). Conventionally, transcriptional terminators were assumed to make up the majority of bacterial 3' UTRs. Nevertheless, transcriptional terminators seldom exceed 40-50 nucleotides in length; hence, 3' UTRs with longer lengths (>100 nt) have been suggested to have additional regulatory elements (Ruiz de los Mozos et al. 2013).

According to new research, 3' UTRs are crucial in controlling gene expression in bacteria (Ren et al. 2017). 3' UTRs, specifically, is able to predict mRNA destabilization (Siegel et al. 2022) and control the speed of mRNA degradation and translational initiation (Maeda and Wachi 2012; Lopez-Garrido et al. 2014; Liu et al. 2016; Zhu et al. 2016). Furthermore, 3' UTRs include a large number of small non-coding RNAs (sRNAs) that can be used to control gene expression selectively (Kim et al. 2014; Tree et al. 2014; Miyakoshi et al. 2015; Chao and Vogel 2016; Peng et al. 2016).

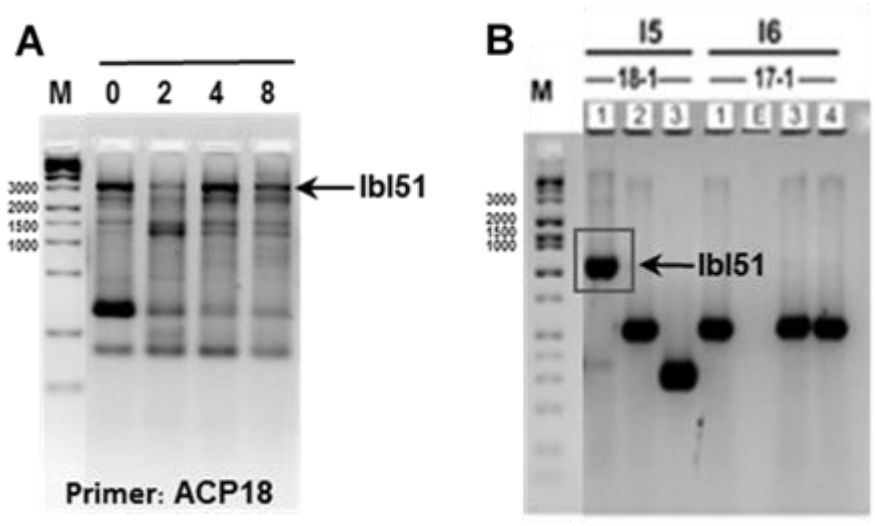

Figure 1. ACP-PCR product using ACP18 and a positive clone *IbI51*. (A) ACP-PCR products of mRNA extracted from non-treated (0 h) sweetpotato storage roots, as well as skinning injury treatment for 2, 4, and (8 + 12) h. The primer ACP18 was used in ACP-PCR. ACP-PCR products that were cut from the gel and cloned are indicated by arrows. Sweetpotato cDNA is displayed in a variety of ways. At 0, 2, 4, and (8 + 12) hours following skinning treatments, GeneFishing revealed amplification products of *IbI51* utilizing ACP arbitrary primer ACP18. (B) The M13 Reverse and M13 Forward universal primers were used to determine the nucleotide sequence of positive cDNA clone *IbI51*. ACP stands for annealing control primer, and M stands for DNA ladder marker. Differentially amplified cDNA bands are marked by arrows

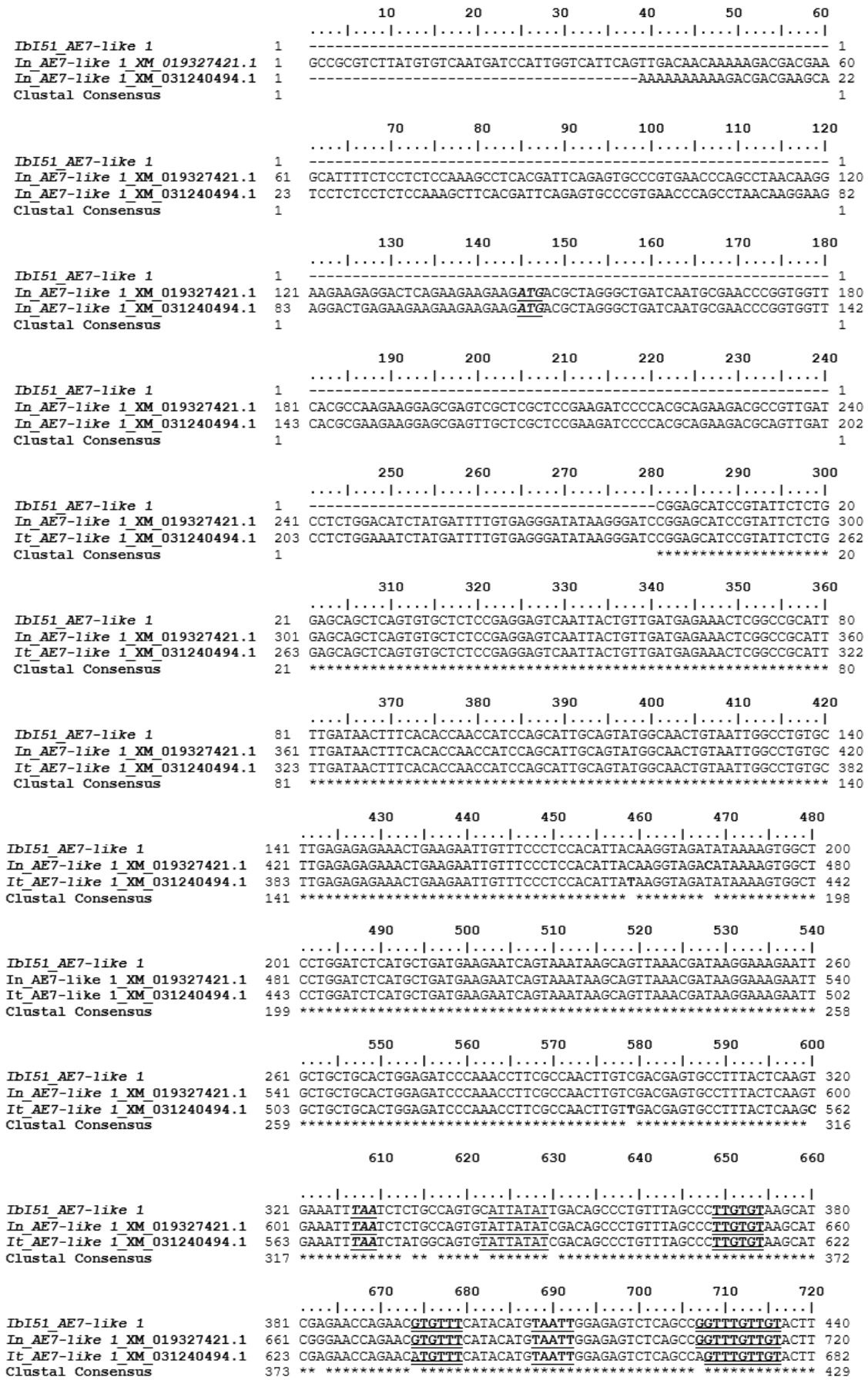
IbI51_AE7-like 1
In_AE7-like 1_XM_019327421.1
In_AE7-like 1_XM_031240494.1
It_AE7-like 1_XM_031240494.1
Clustal Consensus

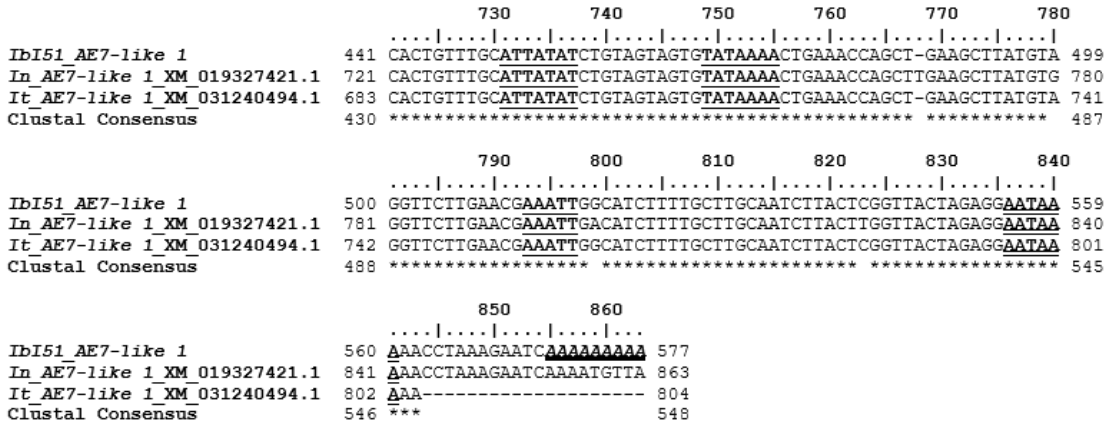

Figure 2. Sequence alignment of *IbAE7-like 1* in response to skinning injury in sweetpotato and *AE7-like 1* from *Ipomoea nil* and *I. triloba*. Star (*) represented same nucleotides, empty space **( )** represented nucleotide differences and dash (-) represented deletions. The codon ***ATG*** is the start codon and the codon ***TAA*** is the stop codon that signal the beginning and the termination of translation, respectively. The consensus polyadenylatìon recognition sequence **AATAAA** is double underlined

Zhao et al. (2018) showed that the addition of an RBS (ribosome binding site) region into 5' end of the 3' UTR of *hmsT, y1235*, and *y4098* genes (from bacteria, mouse, and bacteria, respectively) increased the mRNA levels of all three genes significantly. These findings imply that binding of particular proteins to the 3' UTR, such as ribosomes, can protect it from destruction, hence promoting the stability of upstream mRNA (Castello et al. 2012; Zhao et al. 2018).

The sequence alignment showed that *IbAE7-like 1* has one copy of polyadenylation recognition consensus sequences (AATAAA) that occurred at position 14-18 upstream of the poly (A) site of *AE7-like 1* gene (Figure 2). A similar result by Effendy et al. (2019) showed that *IbSpor* also has one copy of AATAAA hexanucleotide. In contrast, a study by Cole and Stacy (1985) showed that the *thymidine kinase* (*tk*) gene of the herpes simplex virus type 1 has two copies of the AATAAA hexanucleotide.

Figure 2 showed that *IbAE7-like 1* has 3 copies of short GT boxes (6 ─ 10 consecutive residues are G or T) downstream of AATAA sequence and before poly (A) site, while *tk* gene from herpes simplex virus type 1 has a long GT box (18 of 19 consecutive residues are G or T). These GT box previously found to be needed for efficient *tk* mRNA processing and polyadenylation (Cole and Stacy 1985). Besides GT box, *IbAE7-like 1* also has 3 copies of short AT-rich elements (5 ─ 7 consecutive residues are A or T) that caused rapid mRNA degradation (Chen et al. 1995; Barreau et al. 2005).

Mayr (2017) showed that AU-rich regions are found in genes that require strict regulation of their expression, including cytokines, proto-oncogenes, and immune-regulatory proteins (Chen et al. 1995; Barreau et al. 2005). In comparison to the transcriptome's median half-life of 7 hours, these genes had mRNA half-lives of less than 30 minutes (Sharova et al. 2009; Clark et al. 2012; Tani et al. 2012). The importance of these regulatory components in regulating protein production is highlighted by the fact that their absence is connected to cancer, chronic inflammation, and auto-immune disease (Barreau et al. 2005). These findings suggest that effective polyadenylation involves AATAAA as well as downstream GT- and AT-rich regions. Furthermore, sequences at polyadenylation sites and at more distant regions alter processing and polyadenylation in both qualitative and quantitative ways.

Similarity of AE7-like 1 with MIP18, DUF59, FAM96B, and other genes

AE7-like 1 has been isolated from two *Ipomoea* species. The BLASTX search resulted in a total of 100 hits showed that AE7-like 1 was the greatest (58%), followed by MIP18 (8%), DUF59 (2%), and FAM98B (1%). Other proteins such as hypothetical protein (23%), uncharacterized protein (4%), unnamed protein (2%), and unknown function protein (2%) (Figure 3). The AE7 encodes for a protein that belongs to the Domain of Unknown Function 59 (DUF59) family, which has a long evolutionary history (Bernard et al. 2013; Couturier et al. 2013; Mashruwala et al. 2016; Mashruwala and Boyd 2018). Yuan et al. (2010) demonstrated that *AE7* expression was affiliated with proliferating cells in a similar manner to that of the cell cycle marker gene *HISTONE4* and that the DNA repair gene *RAD51* was induced in the *ae7* mutant using the DNA damaging agents: methyl methanesulfonate (MMS) and cisplatin. This study indicated that *AE7* may play a role in DNA replication and/or repair (Yuan et al. 2010). Luo et al. (2012) utilized two *AE7* mutants, *ae7-1* allele (weak ae7) and *ae7-2* allele (strong *ae7*) in their research. The result revealed that the *ae7-1* allele is viable but causes DNA damage, which activates DNA damage responses, causing the cell circle to terminate, whereas the *ae7-2* allele causes embryo death (Luo et al. 2012).

MIP18 is an MMS19 (methyl-methanesulfonate sensitivity 19) that interacts protein 18. MIP18 interacts with both CIAO1 and the Fe-S cluster coordinating area of target Fe-S proteins (marked by the four Cs, for cysteine) (Gari et al. 2012; Stehling et al. 2012). Furthermore, van

Wietmarschen et al. (2012) showed that ADP/ATP translocase 2 (ANT2) bind to this protein complex to aid the insertion of Fe-S clusters into target proteins. The functional Fe-S proteins split from the late acting CIA complex once the Fe-S cluster is inserted. MIP18 and MMS 19 are identified as components of the CIA machinery that play a significant role in Fe-S protein maturation in this model (Gari et al. 2012; Stehling et al. 2012; van Wietmarschen et al. 2012). The family with sequence similarity 96 member B (FAM 96B, also known as MIP18) was sought after as a novel prelamin A binding partner (Ragnauth et al. 2010). Prelamin A accumulation is not seen in young healthy vessels, but it is seen in vascular smooth muscle cells from elderly people, which is associated with nuclear morphology defects (Liu et al. 2013). As a result, toxic accumulation of prelamin A may be a novel target for alleviating the effects of age-related cell dysfunction (Ragnauth et al. 2010). The physical interaction of FAM96B and prelamin A, suggests possible role of FAMB96B on cellular senescence (Xiong et al. 2013). FAM96B was also revealed to be a component of the cytoplasmic Fe-S assembly (CIA) machinery as part of a complex with CIAO1, MMS19, and NARFL, three known CIA system components (Gari et al. 2012; Stehling et al. 2012; van Wietmarschen et al. 2012). These protein complexes have been linked to DNA metabolism, DNA repair, and genomic instability (Gari et al. 2012; Stehling et al. 2012; Shi et al. 2021).

IbAE7-like 1 together with ItAE7-like 1 and InAE7-like 1 encoding AE7-like 1 have four signature cysteine residues, for example, Cys83, Cys92, Cys100, and Cys148 (Figure 4). Multiple sequence alignment shows that the IbAE7-like 1 is missing the first 46 amino acid residues at the 5′ end when compared with AE7-like 1 from *I. nil* and *I. triloba*. However, IbAE7-like 1 has 10 amino acids at the 5′ end at position 37-46 that are unique in *I. batatas* that cannot be found in *I. nil*, *I. triloba* also in AE7-like 1, MIP18, FAM96B and DUF59 from other plants species (Figure 5).

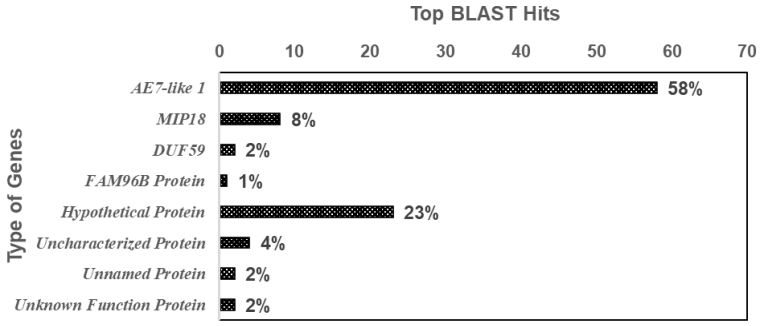

Figure 3. Distribution of genes type and the number of its occurrence in IbAE7-like 1 from sweetpotato in response to skinning injury based on BLASTX 100 hits

```
                                      10        20        30        40        50        60        70
                                      ....|....|....|....|....|....|....|....|....|....|....|....|....|....|
Ib_I51_AE7-like 1              1      ------------------------------------CLPGIRFMGAEHPYSLEQLSVLSEESITVDEKLG 24
In_AE7_2_XP_019182966.1_1      1      MTLGLINANPVVHAKKERVARSEDPHAEDAVDPLDIYDFVRDIRDPEHPYSLEQLSVLSEESITVDEKLG 70
It_AE7_1_XP_031096354.1_1      1      MTLGLINANPVVHAKKERVARSEDPHAEDAVDPLEIYDFVRDIRDPEHPYSLEQLSVLSEESITVDEKLG 70
Clustal Consensus              1                                                ********************** 24

                                      80        90        100       110       120       130       140
                                      ....|....|....|....|....|....|....|....|....|....|....|....|....|....|
Ib_I51_AE7-like 1              25     RILITFTPTIQHCSMATVIGLCLREKLKNCFPPHYKVDIKVAPGSHADEESVNKQLNDKERIAAALEIPN 94
In_AE7_2_XP_019182966.1_1      71     RILITFTPTIQHCSMATVIGLCLREKLKNCFPPHYKVDIKVAPGSHADEESVNKQLNDKERIAAALEIPN 140
It_AE7_1_XP_031096354.1_1      71     RILITFTPTIQHCSMATVIGLCLREKLKNCFPPHYKVDIKVAPGSHADEESVNKQLNDKERIAAALEIPN 140
Clustal Consensus              25     ************************************************************************** 94

                                      150
                                      ....|....|....
Ib_I51_AE7-like 1              95     LRQLVDECLYSSEI 108
In_AE7_2_XP_019182966.1_1      141    LRQLVDECLYSSEI 154
It_AE7_1_XP_031096354.1_1      141    LRQLVDECLYSSEI 154
Clustal Consensus              95     ************** 108
```

Figure 4. The amino acid sequence alignment of IbAE7-like 1 in response to skinning injury in sweetpotato and AE7-like 1 from *Ipomoea nil* and *I. triloba*. Star (*) represented same amino acids, empty space **( )** represented amino acid differences and dash (-) represented deletions

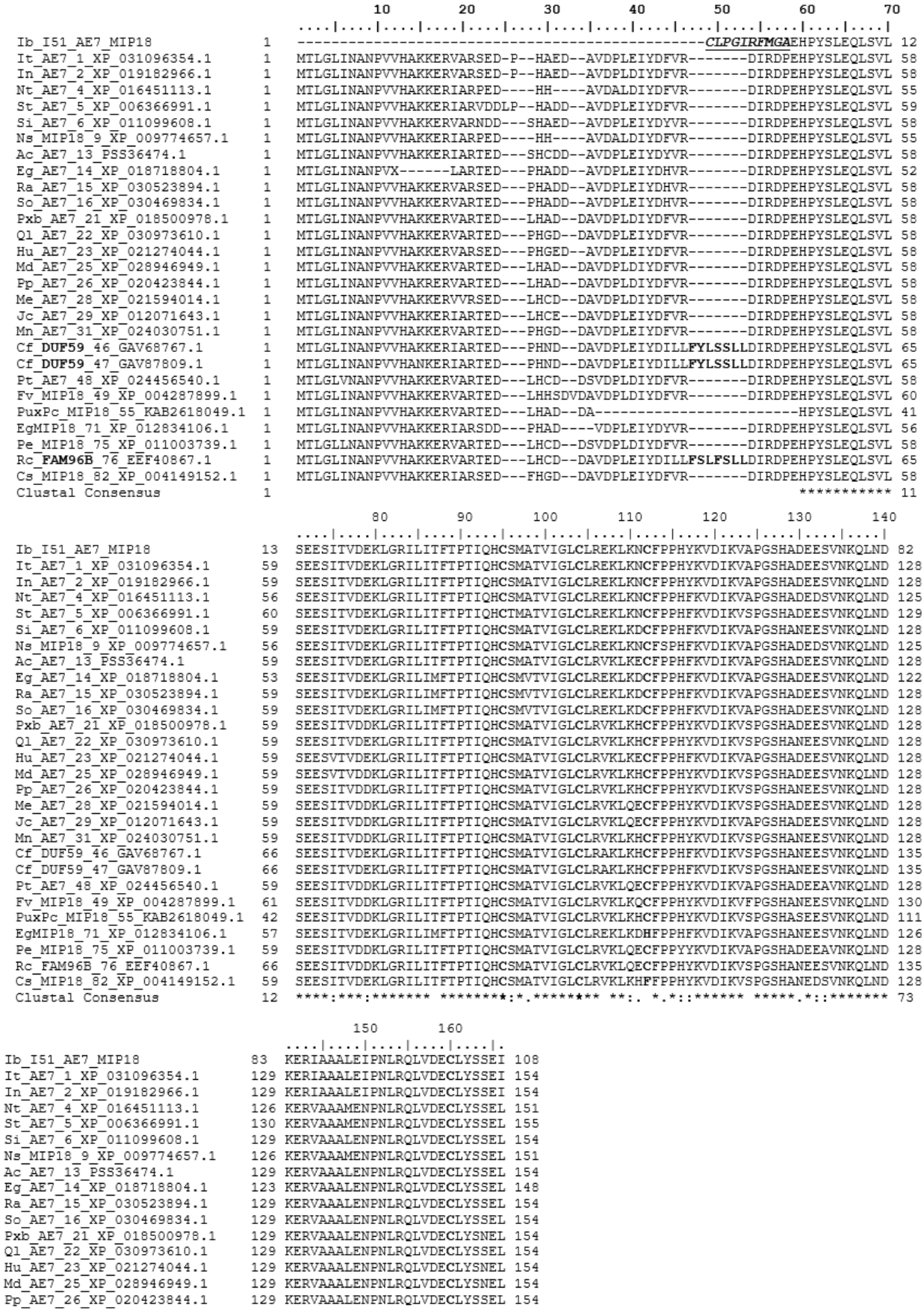
Ib_I51_AE7_MIP18
It_AE7_1_XP_031096354.1
In_AE7_2_XP_019182966.1
Nt_AE7_4_XP_016451113.1
St_AE7_5_XP_006366991.1
Si_AE7_6_XP_011099608.1
Ns_MIP18_9_XP_009774657.1
Ac_AE7_13_PSS36474.1
Eg_AE7_14_XP_018718804.1
Ra_AE7_15_XP_030523894.1
So_AE7_16_XP_030469834.1
Pxb_AE7_21_XP_018500978.1
Ql_AE7_22_XP_030973610.1
Hu_AE7_23_XP_021274044.1
Md_AE7_25_XP_028946949.1
Pp_AE7_26_XP_020423844.1
Me_AE7_28_XP_021594014.1
Jc_AE7_29_XP_012071643.1
Mn_AE7_31_XP_024030751.1
Cf_DUF59_46_GAV68767.1
Cf_DUF59_47_GAV87809.1
Pt_AE7_48_XP_024456540.1
Fv_MIP18_49_XP_004287899.1
PuxPc_MIP18_55_KAB2618049.1
EgMIP18_71_XP_012834106.1
Pe_MIP18_75_XP_011003739.1
Rc_FAM96B_76_EEF40867.1
Cs_MIP18_82_XP_004149152.1
Clustal Consensus

```
Me_AE7_28_XP_021594014.1      129 KERVAAALENPNLRQLVDECLYSSEL 154
Jc_AE7_29_XP_012071643.1      129 KERVAAALENPNLRQLVDECLYSNEL 154
Mn_AE7_31_XP_024030751.1      129 KERVAAALENPNLRQLVDECLYSSEL 154
Cf_DUF59_46_GAV68767.1        136 KERVAAALENPNLRQLVDECLYSNEL 161
Cf_DUF59_47_GAV87809.1        136 KERVAAALENPNLRQLVDECLYSNEL 161
Pt_AE7_48_XP_024456540.1      129 KERVAAALENPNLRQLVDECLYSNEL 154
Fv_MIP18_49_XP_004287899.1    131 KERVAAALENPNLRQLVDECLYSSEL 156
PuxPc_MIP18_55_KAB2618049.1   112 KERIAAALENPNLRQLVDECLYSNEL 137
EgMIP18_71_XP_012834106.1     127 KERVAAALENPNLRQLVDECLYSNEL 152
Pe_MIP18_75_XP_011003739.1    129 KERVAAALENPNLRQLVDECLYSNEL 154
Rc_FAM96B_76_EEF40867.1       136 KERVAAALENPNLRQLVDECLYSNEL 161
Cs_MIP18_82_XP_004149152.1    129 KERVAAAMENPNLRQLVDECLYSSEL 154
Clustal Consensus             74  ***:***:* **********.***.*:
```

Figure 5. The deduced amino acid sequences alignment of IbAE7-like 1, encoded AE7-like 1 from *Ipomoea batatas* (Ib), *I. nil* (In), *I triloba* (It), *Nicotiana tabacum* (Nt), *Solanum tuberosum* (St), *Sesamum indicum* (Si), *Actinidia chinensis var. chinensis* (Ac), *Eucalyptus grandis* (Eg), *Rhodamnia argentea* (Ra), *Syzygium oleosum* (So), *Pyrus x bretschneideri* (Pxb), *Quercus lobate* (Ql), *Herrania umbratica* (Hu), *Malus domestica* (Md), *Prunus persica* (Pp), *Manihot esculenta* (Me), *Jatropha curcas* (Jc), *Morus notabilis* (Mn), *Populus trichocarpa* (Pt); MIP18 from *Nicotiana sylvestris* (Ns), *Fragaria vesca subsp. Vesca* (Fv), *Pyrus ussuriensis x Pyrus communis* (PuxPc), *Erythranthe guttata* (Eg), *Populus euphratica* (Pe), *Cucumis sativus* (Cs); DUF59 from *Cephalotus follicularis* (Cf)**;** FAM96B from *Ricinus communis* (Rc). At the end of each line, the associated GenBank accession numbers are provided. The residues of cysteine are represented by black bold characters on a gray setting

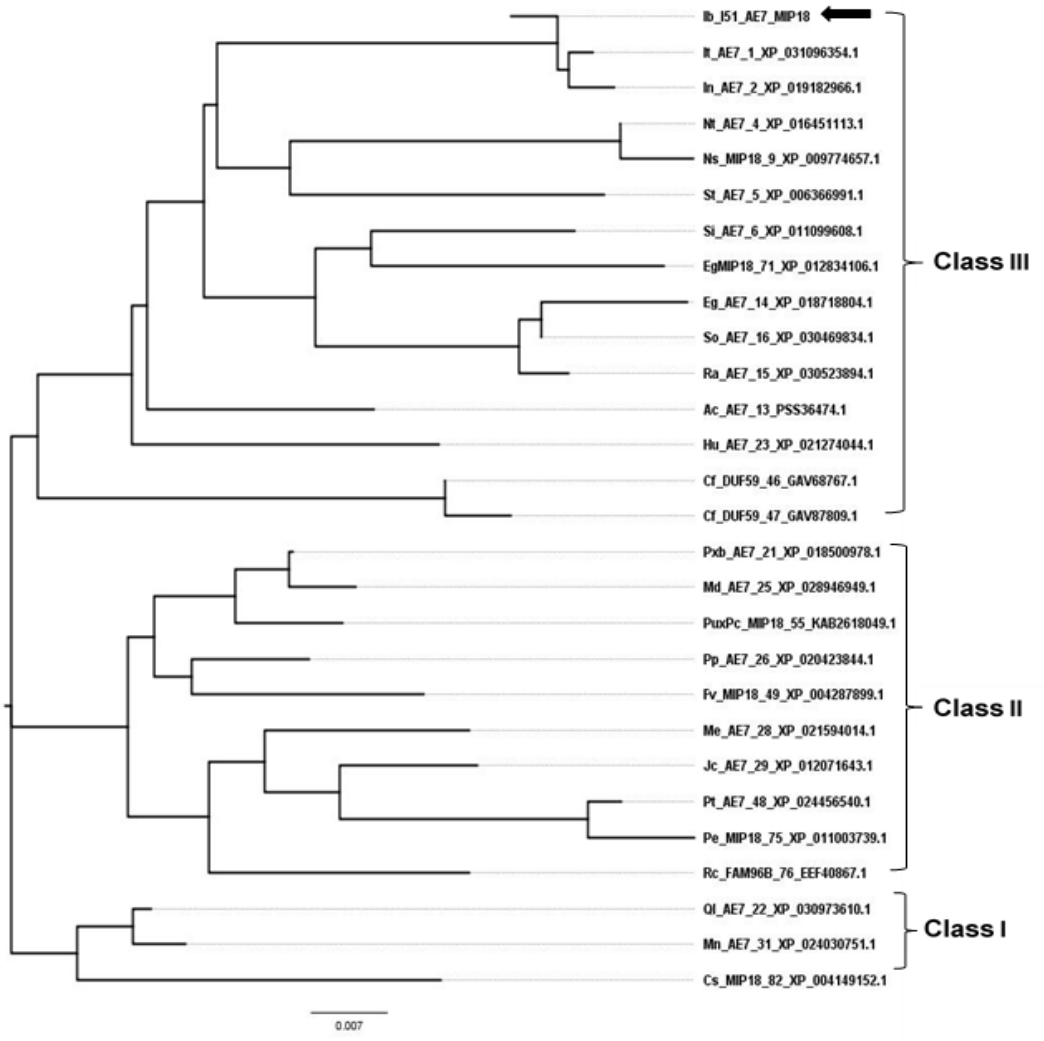

Figure 6. Phylogenetic analysis of the partial amino acid sequence of IbAE7-like 1 with the sequences from other plants. The ClustalX2 program was used to align the amino acid sequences, and FigTree v1.4.3 was used to generate the neighbor-joining tree. The phylogenetic tree provides the respective GenBank accession numbers

In general, multiple sequence alignment shows that IbAE7-like 1, AE7, MIP18, DUF59 and FAM96B have four signature cysteine residues, for example, Cys95, Cys104, Cys112, and Cys160 except for EgMIP18 and CsMIP18 only have 3 Cystein residues (Cys95, Cys104, and Cys160. Cys112 in EgMIP18 is replaced with His (H), while in CsMIP18 is replaced with Phe (P) (Figure 5). Studies by Skryhan et al. (2015) showed that Cys residues have been found to play a crucial role in the stability of protein and the signaling of redox. The conserved, surface-exposed residue R127 in CIA1 is responsible for assembling other subunits of the cytosolic Fe/S protein, according to point mutations (Paul and Lill 2015). The conserved Cys residue, which is likewise conserved in eukaryotes, is essential for CIA2 function (Luo et al. 2012; Stehling et al. 2012). In addition, the maturation of Fe/S proteins is suppressed when human CIA2B or its homolog Cia2 is knocked out (Chen et al. 2012). Other studies by Liu and Huang (2015) showed that DNA Primase2 (PRIM2) comprises four conserved Cys residues: Cys287, Cys367, Cys384, and Cys424, which are critical for coordinating Iron–sulfur (Fe/S) clusters (ISCs). Both PRIM1 and PRIM2 become unstable when point mutation in Cys residues occurred. The unstable structure of PRIM1 and PRIM2 caused the DNA polymerase-α primase complex to malfunction, resulting in a halted replication fork (Liu and Huang 2015). They showed that a single point mutation of the conserved Cys residues is enough to impair DNA primase and DNA polymerase functions. This finding suggests that ISCs play a critical role in enzyme function (Liu and Huang 2015).

Phylogenetic relationship IbAE7-like 1, AE7-like 1 from *Ipomoea* species, and other genes (MIP18, DUF59, FAM96B) from various plant species

The amino acid sequence IbAE7-like 1 was utilized in this research to investigate their phylogenetic relationship with AE7 based on BLASTX available in databases. To examine the relationship between the AE7-like 1 from *Ipomoea* sp. and other related genes from other plant species, an unrooted phylogenetic tree was constructed. As shown in Figure 6, the AE7 proteins from various plants could be divided into three distinct classes (I to III). Class I contained AE7 and MIP18, Class II contained AE7, MIP18 and FAM96B, and Class III contained IbAE7-like 1, AE7, MIP and DUF59. Based on phylogenetic analysis, multiple alignment of IbAE7-like 1 in response to skinning injury, we suggested that AE7-like 1 family members are conserved among *I. batatas*, *I. triloba*, and *I. nil*. Protein sequence sections that are conserved are particularly beneficial for identifying and researching functionally and structurally significant areas. The structural properties of conserved protein sequence areas were revealed using an integrated study of large-scale protein structure and sequence data (Sitbon and Pietrokovski 2007).

In conclusion, the present study provides a novel information about early expression of a skinning injury responsive *AE7-like 1* gene. *IbAE7-like 1* is a part of key proteins involved in CIA Pathway which function in stabilizing their structures as well as coordinating their local conformational changes, and promoting DNA charge transport. Enhanced our understanding of CIA pathways' crucial involvement in DNA replication and repair enzymes will eventually help us solve the huge riddles surrounding the DNA metabolism enzymes related to postharvest loss due to skinning injury that is particularly high in developing and underdeveloped countries.

ACKNOWLEDGEMENTS

Funding for this sweetpotato research was provided by Borlaug Fellowship from the United State Department of Agriculture, Foreign Agricultural Service to JE.

REFERENCES

Altschul SF, Madden TL, Schaffer AA, Zhang J, Zhang Z, Miller W, Lipman DJ. 1997. Gapped BLAST and PSI-BLAST: A new generation of protein database search programs. Nucleic Acids Res 25 (17): 3389-3402. DOI: 10.1093/nar/25.17.3389.

Andreini C, Rosato A, Banci L. 2017. The relationship between environmental dioxygen and iron-sulfur proteins explored at the genome level. PLoS ONE 12 (1): e0171279. DOI: 10.1371/journal.pone.0171279.

Babajani G, Effendy J, Plant AL. 2009. *Sl-SROl1* increases salt tolerance and is a member of the *radical-induced cell death 1—similar* to *RCD1* gene family of tomato. Plant Sci 176 (2): 214-222. DOI: 10.1016/j.plantsci.2008.10.012.

Baichoo Z, Jaufeerally-Fakim Y. 2016. Identification and analysis of differentially expressed genes in *Solanum* lines in response to challenge with a *Ralstonia solanacearum* phylotype I strain. Plant Gene 8: 1-8. DOI: 10.1016/j.plgene.2016.09.002.

Barreau C, Paillard L, Osborne HB. 2005. AU-rich elements and associated factors: are there unifying principles?. Nucleic Acids Res 33 (22): 7138-7150. DOI: 10.1093/nar/gki1012.

Bernard DG, Netz DJ, Lagny TJ, Pierik AJ, Balk J. 2013. Requirements of the cytosolic iron-sulfur cluster assembly pathway in Arabidopsis. Phil Trans R Soc B 368 (1622): 20120259. DOI: 10.1098/rstb.2012.0259.

Castello A, Fischer B, Eichelbaum K, Horos R, Beckmann BM, Strein C, Davey NE, Humphreys DT, Preiss T, Steinmetz LM. 2012. Insights into RNA biology from an atlas of mammalian mRNA-binding proteins. Cell 149 (6): 1393-1406. DOI: 10.1016/j.cell.2012.04.031.

Chao Y, Vogel J. 2016. A 3' UTR-derived small RNA provides the regulatory noncoding arm of the inner membrane stress response. Mol Cell 61 (3): 352-363. DOI: 10.1016/j.molcel.2015.12.023.

Chen CY, Shyu AB. 1995. AU-rich elements: characterization and importance in mRNA degradation. Trends Biochem Sci 20 (11): 465-470. DOI: 10.1016/s0968-0004(00)89102-1.

Chen KE, Richards AA, Ariffin JK, Ross IL, Sweet MJ, Kellie S, Kobe B, Martin JL. 2012. The mammalian DUF59 protein Fam96a forms two distinct types of domain-swapped dimer. Acta Crystallogr D Biol Crystallogr 68: 637-648. DOI: 10.1107/S0907444912006592.

Clark MB, Johnston RL, Inostroza-Ponta M, Fox AH, Fortini E, Moscato P, Dinger ME, Mattick JS. 2012. Genome-wide analysis of long noncoding RNA stability. Genome Res 22 (5): 885-898. DOI: 10.1101/gr.131037.111.

Cole CN, Stacy TP. 1985. Identification of sequences in the herpes simplex virus thymidine kinase gene required for efficient processing and polyadenylation. Mol Cell Biol 5 (8): 2104-2113. DOI: 10.1128/mcb.5.8.2104-2113.1985.

Couturier J, Touraine B, Briat JF, Gaymard F, Rouhier N. 2013. The iron-sulfur cluster assembly machineries in plants: Current knowledge and open questions. Front Plant Sci 4: 259. DOI: 10.3389/fpls.2013.00259.

Effendy J, La Bonte DR, Baisakh N. 2013. Identification and expression of skinning injury-responsive genes in sweetpotato. J Amer Soc Hort Sci 138 (3): 210-216. DOI: 10.21273/jashs.138.3.210.

Effendy J, LaBonte DR, Efendi D. 2019. Isolation and characterization of cDNA clones encoding a novel subfamily sporamin B in sweet potato. Biodiversitas 20 (10): 3033-3041. DOI: 10.13057/biodiv/d201036.

Fuss JO, Tsai CL, Ishida JP, Tainer JA. 2015. Emerging critical roles of Fe-S clusters in DNA replication and repair. Biochim Biophys Acta 1853 (6): 1253-1271. DOI: 10.1016/j.bbamcr.2015.01.018.

Gari K, Ortiz AML, Borel V, Flynn H, Skehel JM, Boulton SJ. 2012. MMS19 links cytoplasmic iron-sulfur cluster assembly to DNA metabolism. Science 337 (6091): 243-245. DOI: 10.1126/science.1219664.

Hall TA. 1999. BioEdit: A user-friendly biological sequence alignment editor and analysis program for Windows 95/98/NT. Paper read at Nucleic Acids Symp Ser.

Huang YJ, Zhou Q, Huang JQ, Zeng YR, Wang ZJ, Zhang QX, Zhu YH, Shen C, Zheng BS. 2015. Transcriptional profiling by DDRT-PCR analysis reveals gene expression during seed development in *Carya cathayensis* Sarg. Plant Physiol Biochem 91: 28-35. DOI: 10.1016/j.plaphy.2015.03.008.

Hwang IT, Kim YJ, Kim SH, Kwak CI, Gu YY, Chun JY. 2003. Annealing control primer system for improving specificity of PCR amplification. BioTechniques 35 (6): 1180-1184. DOI: 10.2144/03356st03.

Hwang SJ, Lee HJ. 2021. Identification of differentially expressed genes in mouse embryonic stem cell under hypoxia. Genes Genom 43 (4): 313-321. DOI: 10.1007/s13258-020-01009-4.

Kim HM, Shin JH, Cho YB, Roe JH. 2014. Inverse regulation of Fe- and Ni-containing SOD genes by a Fur family regulator Nur through small RNA processed from 3'UTR of the *sodF* mRNA. Nucleic Acids Res 42 (3): 2003-2014. DOI: 10.1093/nar/gkt1071.

Laalami S, Zig L, Putzer H. 2014. Initiation of mRNA decay in bacteria. Cell Mol Life Sci 71 (10): 1799-1828. DOI: 10.1007/s00018-013-1472-4.

Lanz ND, Booker SJ. 2012. Identification and function of auxiliary iron-sulfur clusters in radical SAM enzymes. Biochim Biophys Acta 1824 (11): 1196-1212. DOI: 10.1016/j.bbapap.2012.07.009.

Larkin MA, Blackshields G, Brown NP, Chenna R, McGettigan PA, McWilliam H, Valentin F, Wallace IM, Wilm A, Lopez R, Thompson JD, Gibson TJ, Higgins DG. 2007. Clustal W and Clustal X version 2.0. Bioinformatics 23 (21): 2947-2948. DOI: 10.1093/bioinformatics/btm404.

Lee K-W, Kim K-H, Kim Y-G, Lee BH, Lee S-H. 2012. Identification of *MsHsp23* gene using annealing control primer system. Acta Physiol Plant 34 (2): 807-811. DOI: 10.1007/s11738-011-0853-2.

Lill R, Broderick JB, Dean DR. 2015a. Special issue on iron-sulfur proteins: Structure, function, biogenesis and diseases. Biochim Biophys Acta 1853(6): 1251-1252. DOI: 10.1016/j.bbamcr.2015.03.001.

Lill R, Dutkiewicz R, Freibert SA, Heidenreich T, Mascarenhas J, Netz DJ, Paul VD, Pierik AJ, Richter N, Stumpfig M, Srinivasan V, Stehling O, Muhlenhoff U. 2015b. The role of mitochondria and the CIA machinery in the maturation of cytosolic and nuclear iron-sulfur proteins. Eur J Cell Biol 94 (7-9): 280-291. DOI: 10.1016/j.ejcb.2015.05.002.

Lill R, Freibert SA. 2020. Mechanisms of mitochondrial iron-sulfur protein biogenesis. Annu Rev Biochem 89 (9): 471-499. DOI: 10.1146/annurev-biochem-013118-111540.

Lill R. 2020. From the discovery to molecular understanding of cellular iron-sulfur protein biogenesis. Biol Chem 401 (6-7): 855-876. DOI: 10.1515/hsz-2020-0117.

Liu B, Kearns DB, Bechhofer DH. 2016. Expression of multiple *Bacillus subtilis* genes is controlled by decay of *slrA* mRNA from Rho-dependent 3' ends. Nucleic Acids Res 44 (7): 3364-3372. DOI: 10.1093/nar/gkw069.

Liu L, Huang M. 2015. Essential role of the iron-sulfur cluster binding domain of the primase regulatory subunit Pri2 in DNA replication initiation. Protein Cell 6 (3): 194-210. DOI: 10.1007/s13238-015-0134-8.

Liu Y, Drozdov I, Shroff R, Beltran LE, Shanahan CM. 2013. Prelamin A accelerates vascular calcification via activation of the DNA damage response and senescence-associated secretory phenotype in vascular smooth muscle cells. Circul Res 112 (10): e99-e109. DOI: 10.1161/CIRCRESAHA.111.300543.

Lopez-Garrido J, Puerta-Fernandez E, Casadesus J. 2014. A eukaryotic-like 3' untranslated region in *Salmonella enterica hilD* mRNA. Nucleic Acids Res 42 (9): 5894-5906. DOI: 10.1093/nar/gku222.

Luo D, Bernard DG, Balk J, Hai H, Cui X. 2012. The DUF59 family gene *AE7* acts in the cytosolic iron-sulfur cluster assembly pathway to maintain nuclear genome integrity in *Arabidopsis*. Plant Cell 24 (10): 4135-4148. DOI: 10.1105/tpc.112.102608.

Maeda T, Wachi M. 2012. 3' Untranslated region-dependent degradation of the *aceA* mRNA, encoding the glyoxylate cycle enzyme isocitrate lyase, by RNase E/G in *Corynebacterium glutamicum*. Appl Environ Microbiol 78 (24): 8753-8761. DOI: 10.1128/AEM.02304-12.

Mashruwala AA, Bhatt S, Poudel S, Boyd ES, Boyd JM. 2016. The DUF59 containing protein SufT Is involved in the maturation of iron-sulfur (FeS) proteins during conditions of high FeS cofactor demand in *Staphylococcus aureus*. PLoS Genet 12 (8): e1006233. DOI: 10.1371/journal.pgen.1006233.

Mashruwala AA, Boyd JM. 2018. Investigating the role(s) of SufT and the domain of unknown function 59 (DUF59) in the maturation of iron-sulfur proteins. Curr Genet 64 (1): 9-16. DOI: 10.1007/s00294-017-0716-5.

Mayr C. 2017. Regulation by 3'-untranslated regions. Annu Rev Genet 51 (1): 171-194. DOI: 10.1146/annurev-genet-120116-024704.

Miyakoshi M, Chao Y, Vogel J. 2015. Regulatory small RNAs from the 3' regions of bacterial mRNAs. Curr Opin Microbiol 24: 132-139. DOI: 10.1016/j.mib.2015.01.013.

Paul VD, Lill R. 2015. Biogenesis of cytosolic and nuclear iron-sulfur proteins and their role in genome stability. Biochim Biophys Acta 1853 (6): 1528-1539. DOI: 10.1016/j.bbamcr.2014.12.018.

Peng T, Berghoff BA, Oh JI, Weber L, Schirmer J, Schwarz J, Glaeser J, Klug G. 2016. Regulation of a polyamine transporter by the conserved 3' UTR-derived sRNA SorX confers resistance to singlet oxygen and organic hydroperoxides in *Rhodobacter sphaeroides*. RNA Biol 13 (10): 988-999. DOI: 10.1080/15476286.2016.1212152.

Piccioli M. 2018. The biogenesis of iron–sulfur proteins: from cellular biology to molecular aspects. J Biol Inorg Chem 23 (4): 493-494. DOI: 10.1007/s00775-018-1555-7.

Ragnauth CD, Warren DT, Liu Y, McNair R, Tajsic T, Figg N, Shroff R, Skepper J, Shanahan CM. 2010. Prelamin A acts to accelerate smooth muscle cell senescence and is a novel biomarker of human vascular aging. Circulation 121 (20): 2200-2210. DOI: 10.1161/CIRCULATIONAHA.109.902056.

Rambaut A. 2017. FigTree-version 1.4. 3, a graphical viewer of phylogenetic trees. Computer program distributed by the author. http://tree bio ed ac uk/software/figtree.

Ren GX, Guo XP, Sun YC. 2017. Regulatory 3' untranslated regions of bacterial mRNAs. Front Microbiol 8: 1276. DOI: 10.3389/fmicb.2017.01276.

Ruiz de los Mozos I, Vergara-Irigaray M, Segura V, Villanueva M, Bitarte N, Saramago M, Domingues S, Arraiano CM, Fechter P, Romby P, Valle J, Solano C, Lasa I, Toledo-Arana A. 2013. Base pairing interaction between 5'- and 3'-UTRs controls *icaR* mRNA translation in *Staphylococcus aureus*. PLoS Genet 9 (12): e1004001. DOI: 10.1371/journal.pgen.1004001.

Sharova LV, Sharov AA, Nedorezov T, Piao Y, Shaik N, Ko MS. 2009. Database for mRNA half-life of 19 977 genes obtained by DNA microarray analysis of pluripotent and differentiating mouse embryonic stem cells. DNA Res 16 (1): 45-58. DOI: 10.1093/dnares/dsn030.

Shi R, Hou W, Wang ZQ, Xu X. 2021. Biogenesis of iron-sulfur clusters and their role in DNA metabolism. Front Cell Dev Biol 9 (2676): 735678. DOI: 10.3389/fcell.2021.735678.

Siegel DA, Le Tonqueze O, Biton A, Zaitlen N, Erle DJ. 2022. Massively parallel analysis of human 3′ UTRs reveals that AU-rich element length and registration predict mRNA destabilization. G3 12 (1): jkab404. DOI: 10.1093/g3journal/jkab404.

Sitbon E, Pietrokovski S. 2007. Occurrence of protein structure elements in conserved sequence regions. BMC Struct Biol 7: 3. DOI: 10.1186/1472-6807-7-3.

Skryhan K, Cuesta-Seijo JA, Nielsen MM, Marri L, Mellor SB, Glaring MA, Jensen PE, Palcic MM, Blennow A. 2015. The role of cysteine residues in redox regulation and protein stability of *Arabidopsis thaliana* starch synthase 1. PLoS ONE 10 (9): e0136997. DOI: 10.1371/journal.pone.0136997.

Song J, Niu Z, Li Q, Bao Y, Ma X, Wang H, Kong L, Feng D. 2014. Isolation and identification of differentially expressed genes from wheat in response to *Blumeria graminis* f. sp. *tritici* (*Bgt*). Plant Mol Biol Rep 33 (5): 1371-1380. DOI: 10.1007/s11105-014-0838-6.

Srivastava S, Gupta SM, Sane AP, Nath P. 2012. Isolation and characterization of ripening related pectin methylesterase inhibitor

gene from banana fruit. Physiol Mol Biol Plants 18 (2): 191-195. DOI: 10.1007/s12298-012-0102-1.

Stehling O, Vashisht AA, Mascarenhas J, Jonsson ZO, Sharma T, Netz DJ, Pierik AJ, Wohlschlegel JA, Lill R. 2012. MMS19 assembles iron-sulfur proteins required for DNA metabolism and genomic integrity. Science 337 (6091): 195-199. DOI: 10.1126/science.1219723.

Tani H, Mizutani R, Salam KA, Tano K, Ijiri K, Wakamatsu A, Isogai T, Suzuki Y, Akimitsu N. 2012. Genome-wide determination of RNA stability reveals hundreds of short-lived noncoding transcripts in mammals. Genome Res 22 (5): 947-956. DOI: 10.1101/gr.130559.111.

Tree JJ, Granneman S, McAteer SP, Tollervey D, Gally DL. 2014. Identification of bacteriophage-encoded anti-sRNAs in pathogenic *Escherichia coli*. Mol Cell 55 (2): 199-213. DOI: 10.1016/j.molcel.2014.05.006.

van Wietmarschen N, Moradian A, Morin GB, Lansdorp PM, Uringa EJ. 2012. The mammalian proteins MMS19, MIP18, and ANT2 are involved in cytoplasmic iron-sulfur cluster protein assembly. J Biol Chem 287 (52): 43351-43358. DOI: 10.1074/jbc.M112.431270.

Wang BH, Sun XX, Dong FY, Zhang F, Niu JX. 2014. Cloning and expression analysis of an MYB gene associated with calyx persistence in Korla fragrant pear. Plant Cell Rep 33 (8): 1333-1341. DOI: 10.1007/s00299-014-1619-2.

Wei J, Tirajoh A, Effendy J, Plant AL. 2000. Characterization of salt-induced changes in gene expression in tomato (*Lycopersicon esculentum*) roots and the role played by abscisic acid. Plant Sci 159 (1): 135-148. DOI: 10.1016/s0168-9452(00)00344-7.

Xiong XD, Wang J, Zheng H, Jing X, Liu Z, Zhou Z, Liu X. 2013. Identification of FAM96B as a novel prelamin A binding partner. Biochem Biophys Res Commun 440 (1): 20-24. DOI: 10.1016/j.bbrc.2013.08.099.

Yuan Z, Luo D, Li G, Yao X, Wang H, Zeng M, Huang H, Cui X. 2010. Characterization of the *AE7* gene in *Arabidopsis* suggests that normal cell proliferation is essential for leaf polarity establishment. Plant J 64 (2): 331-342. DOI: 10.1111/j.1365-313X.2010.04326.x.

Zhao JP, Zhu H, Guo XP, Sun YC. 2018. AU-rich long 3' untranslated region regulates gene expression in bacteria. Front Microbiol 9: 3080. DOI: 10.3389/fmicb.2018.03080.

Zhu H, Mao XJ, Guo XP, Sun YC. 2016. The *hmsT* 3' untranslated region mediates c-di-GMP metabolism and biofilm formation in *Yersinia pestis*. Mol Microbiol 99 (6): 1167-1178. DOI: 10.1111/mmi.13301.